Indices to be used in comparison of UKCP18 and EuroCORDEX ensembles

Project CR20-3: Enabling the use and producing improved understanding of EuroCORDEX data over the UK

Clair Barnes
Department of Statistical Science, UCL

Richard Chandler[1]
Department of Statistical Science, UCL

Chris Brierley
Geography Department, UCL

July 2022

[1]Please direct all communications to richard.chandler@ucl.ac.uk

Contents

1 Introduction

The UK Climate Projections (UKCP) provide a number of different products that provide information about the future climate of the UK, including Global (60km), regional (12km) and local (2.2km) model projections. While the regional simulations are proving beneficial in understanding future climate risks to the UK (for example, Kennedy-Asser et al., 2021; Arnell et al., 2021), these were driven only by a subset of global climate models (GCMs) based on HadGEM3-GC3, and so may not sample as full a range of uncertainty as desirable. The aim of Project CR20-3 is to complement the UKCP 12km regional climate model (RCM) simulations by combining them with information from the EuroCORDEX climate projections. This combined set will allow a better understanding of structural uncertainty in UK climate projections (Murphy et al., 2018; Arnell et al., 2021) and will provide many additional realisations of future RCM climate for the UK and support future climate change risk assessments.

The first stage of this project aims to analyse and understand the EuroCORDEX results (both the GCM and the RCM components) over the UK region, presenting results for the period from 1980 to 2080, and comparing these with the Global and Regional components of UKCP. The analysis will initially focus on the core indices available for UKCP global and regional simulations including air temperature, precipitation, surface pressure, humidity, surface winds, cloud amount and surface short and long wave radiation (Fung et al., 2018, see Table C1), and will provide information at daily, monthly, seasonal and annual time scales. Additional indices will be used to characterise potential sector impacts that are relevant for drought, flood, agriculture, energy demand, health, infrastructure and transportation, in order to develop an understanding of current and future UK climate risks. This report summarises the proposed indices that will be used to evaluate and characterise the EuroCORDEX model output alongside the UKCP18 projections. The analysis will be divided into two Key Areas:

KA1 – characteristics of internal climate variability

The selected indices will include those produced within UKCP to provide a basis for comparison, alongside a broader range of indices intended to support risk assessment and adaptation planning in a variety of sectors.

KA2 – physical plausibility

The indices for KA2 will be measures of key physical modes of variability. A comparison with observed indices will provide insights into the large-scale physical realism of the models: it will also help to support the evaluation of linked risks, for example from multiple weather phenomena or from simultaneous hazards at multiple spatial locations, for which large-scale and inter-variable relationships are important.

All indices will be computed for each individual simulation in the combined UKCP-EuroCORDEX archive. This archive has a hierarchical structure, with several RCMs being driven by each individual GCM; and, in turn, several GCMs being run for each representative concentration pathway (RCP). All indices will be computed at each level of this hierarchy, so that results for specified representative concentration pathways (RCPs) will also be available for each RCM or GCM family. The same indices will be computed for the gridded HadUK-Grid observations and ERA5 reanalysis data, and made publicly available. Indices will be computed for each grid square (at spatial scales corresponding to both the global and regional UKCP projections) and also for defined spatial regions, and at monthly, seasonal and annual scales as appropriate. All indices will be computed for future periods under RCP8.5 and for various global warming levels.

2 Internal climate variability (KA1)

Data from the UKCP18 projections are publicly available for the fifteen core variables listed in Table C1 in Appendix C (Fung et al., 2018). Monthly, seasonal and annual means of these variables will be computed for the EuroCORDEX simulations and made available in the same format as the UKCP18 data. This report describes the additional indices that will be used to explore the distribution of the simulated weather variables.

Indices of single weather variables were selected from among the CLIMDEX indices used by the World Meteorological Organisation (WMO) to characterise extreme heat, cold and precipitation (Klein Tank et al., 2009); from the expanded set of indices used by the European Climate Assessment & Dataset project (ECA&D, 2020); and from the measures of more extreme weather phenomena proposed by the EU COST action VALUE (Maraun et al., 2015). A number of derived indices, measuring the combined effects of two or more variables, were also included after consultation with stakeholders over impact-relevant indices.

The additional indices are described in Sections 2.1-2.4 below. Each section begins with a description of the indices and their purpose, then provides a precise definition of each index. Some of the proposed indices are only meaningful at certain timescales; tables summarising the proposed indices, along with the temporal resolutions at which they will be reported, are provided in Appendix C.

No bias correction will be carried out before computing the indices. This means that where fixed thresholds are used - for example, in identifying cold spells, which are defined according to Public Health England's guidance as periods of two or more days during which the daily mean temperature falls below 2°C - different models may display different biases; the magnitude and effect of these biases will be considered in a later stage of the project, as part of the process of quantifying the uncertainty in the simulations. Where climatological thresholds are used - as, for example, when identifying cold nights on which the daily minimum temperature falls below the 10th percentile of the distribution of minimum temperatures during the reference period 1981–2010 - the thresholds for each simulation will be based on that simulation's internal climatology. Users should note that, while summaries of the EuroCORDEX data will be provided for the same twenty- and thirty-year time slices already available for the UKCP18 data, the reference period used throughout is not the same as that used in the original UKCP18 analysis, which used a twenty-year reference period. Instead, reporting will use thirty-year time-slices as recommended by the World Meteorological Organisation (WMO, 2017), reflecting the potential interest in these results to a wider international audience, with the reference period running from December 1st 1980 to November 30th 2010.

2.1 Descriptive indices of temperature

Surface air temperature is a key indicator of climate change, with both unusually high and unusually low temperatures having implications for human health (Hajat et al., 2014), energy demand (Wood et al., 2015; Azevedo et al., 2015) and critical infrastructure (Palin et al., 2013). Risks associated with extremes of temperature are typically exacerbated when these extremes are sustained (Meehl and Tebaldi, 2004); the indices considered here therefore characterise not only the range of daily temperatures, but also the persistence and frequency of unusually high or low temperatures.

Mean temperatures form part of the core set of indices listed in Table C1. In addition, the hottest and coldest temperatures in each period will be derived from the corresponding daily maxima and

minima. Changes in the frequency of moderately extreme temperatures will be assessed using 'day-count' indices, as recommended by Klein Tank et al. (2009). For example, the number of cold nights is defined as the number of occurrences of the minimum daily temperature falling below the 10th percentile of the climatological distribution of the reference period (1981–2010); counts of cold days, and warm days and nights, are defined similarly (see precise definitions below). In addition to indices based on percentile thresholds, software will be provided to calculate exceedances of absolute thresholds (for example, icing days where the maximum daily temperature is below zero, or tropical nights where the minimum temperature is greater than 20°C).

The frequency of potentially high-impact long-lasting extreme temperature events is represented by counts of the number of days in heatwaves and cold spells of more than two days' duration; the definitions used are based on the thresholds used by Public Health England (PHE) to initiate heatwave or cold weather plans (PHE, 2020, 2018). Software will also be provided for the computation of such 'spell-count' indices with user-specified thresholds and durations to support future impact studies.

Spatially aggregated indices of temperature will not be reported, but software will be provided to calculate indices over defined regions for users that require this facility.

2.1.1 Definitions of temperature indices

In defining the following indices of temperature, let $\texttt{tas}_{ij}$ be the daily mean temperature on day i in period j; the daily minimum and maximum temperature on day i in period j are denoted by $\texttt{tasmin}_{ij}$ and $\texttt{tasmax}_{ij}$ respectively.

Peak temperature: The highest daily temperature simulated in period j is $\max(\texttt{tasmax}_{ij})$ (Klein Tank et al., 2009).

Temperature nadir: The lowest daily temperature simulated in period j is $\min(\texttt{tasmin}_{ij})$ (Klein Tank et al., 2009).

Number of cold nights: Let $q_{10}(\texttt{tasmin}_{ir})$ be the 10th percentile of daily minimum temperature calculated for a five-day window centred on calendar day i in the reference period r (1981–2010). Count the number of days where $\texttt{tasmin}_{ij} < q_{10}(\texttt{tasmin}_{ir})$ (Klein Tank et al., 2009).

Number of cold days: Let $q_{10}(\texttt{tasmax}_{ir})$ be the c10th percentile of daily maximum temperature calculated for a five-day window centred on calendar day i in the reference period r (1981–2010). Count the number of days where $\texttt{tasmax}_{ij} < q_{10}(\texttt{tasmax}_{ir})$ (Klein Tank et al., 2009).

Number of warm nights: Let $q_{90}(\texttt{tasmin}_{ir})$ be the 90th percentile of daily minimum temperature calculated for a five-day window centred on calendar day i in the reference period r (1981–2010). Count the number of days where $\texttt{tasmin}_{ij} > q_{90}(\texttt{tasmin}_{ir})$ (Klein Tank et al., 2009).

Number of warm days: Let $q_{90}(\texttt{tasmax}_{ir})$ be the 90th percentile of daily maximum temperature calculated for a five-day window centred on calendar day i in the reference period r (1981–2010). Count the number of days where $\texttt{tasmax}_{ij} > q_{90}(\texttt{tasmax}_{ir})$ (Klein Tank et al., 2009).

Duration of heatwaves: Count the number of days where $\texttt{tasmax}_{ij} > t_1$ and $\texttt{tasmin}_{ij} > t_2$ for two or more consecutive days, where t_1 and t_2 are thresholds defined for each region as in Table 1 (PHE, 2020).

Table 1: Thresholds t_1 (daytime temperature) and t_2 (nighttime temperature) in °C used in the PHE (2020) to define a heatwave in each of the administrative regions defined in Fung et al. (2018).

Region	t_1	t_2	Region	t_1	t_2
London	32	18	North East England	28	15
South East England	31	16	Isle of Man	30	15
South West England	30	15	Channel Islands	30	15
East of England	30	15	Wales	30	15
West Midlands	30	15	East Scotland	28	15
East Midlands	30	15	West Scotland	28	15
North West England	30	15	North Scotland	28	15
Yorkshire and Humber	29	15	Northern Ireland	28	15

Duration of cold spells: Count the number of days where $\texttt{tas}_{ij} < 2$°C for more than two consecutive days (PHE, 2018).

Diurnal temperature range The average diurnal temperature range in period j is the difference between the average of $\texttt{tasmax}_{ij}$ and the average of $\texttt{tasmin}_{ij}$ in period j.

1st percentile of daily mean near-surface air temperatures: addThis index can only be computed for extended time periods. The daily mean temperatures $\texttt{tas}_{ij}$ during the season of interest j for all years in the selected time period are pooled, and the 1st percentile of the pooled seasonal temperatures is calculated.

99th percentile of daily mean near-surface air temperatures: addThis index can only be computed for extended time periods. The daily mean temperatures $\texttt{tas}_{ij}$ during the season of interest j for all years in the selected time period are pooled, and the 99th percentile of the pooled seasonal temperatures is calculated.

Seasonal temperature range The seasonal temperature range in period j is the difference between the 99th and 1st percentiles of $\texttt{tas}_{ij}$ in that period.

2.2 Descriptive indices of precipitation

Flooding is currently one of the most socially and economically disruptive natural hazards in the UK (Hurford et al., 2012); to understand the changing risks from changing patterns of precipitation, it is necessary to consider not only short, intense periods of rainfall, but also the duration and intensity of sustained rainfall, and the accumulated precipitation over larger areas (Maraun et al., 2015).

Any day with more than 1mm total precipitation will be classified as a wet day, following Klein Tank et al. (2009) and ECA&D (2020); further analysis will be carried out to confirm that this is an appropriate threshold for all models. For each period the simple daily intensity index (mean wet-day precipitation) will be reported, along with the total precipitation, maximum one-day precipitation and maximum precipitation falling in any five consecutive days ending in that period. Software will be made available to allow users to compute the number of days on which the total precipitation exceeds a given threshold, and also the total precipitation on days exceeding a given threshold.

Precipitation resulting from convective processes may have different implications for warning systems to precipitation resulting from frontal processes; the proportion of total precipitation resulting from convective processes will therefore also be reported.

The fraction of wet days in a period captures trends in the overall frequency of dry and wet days.

However, many impacts are sensitive to both quantity and timing of precipitation, so it is particularly important that the the simulations contain realistic temporal patterns of wet and dry days. To this end, the mean and maximum lengths of dry and wet spells will be reported for each period (Maraun et al., 2015; ECA&D, 2020), along with the relative probabilities of a wet day being succeeded by a wet day, and a dry day being succeeded by a dry day. These 'wet-dry transition probabilities' provide an index of the persistence of wet and dry weather respectively.

Similarly, floods may be caused by extremely high rainfall over a small area, but may also result from moderate precipitation over a larger area. Model-based approaches to describing spatial structure in the simulated precipitation may be used to quantify correlation between rainfall amounts in nearby grid cells (Maraun et al., 2015); however, such approaches generally evaluate correlations over straight-line distances that may not reflect physically meaningful areas, and the resulting models can be difficult to interpret in a meaningful way. The hydrometric areas defined by the Centre for Ecology and Hydrology (CEH: National River Flow Archive, 2014, see Figure B1) will be used to define regions within which simultaneous heavy precipitation might be expected to cause flooding. The mean and maximum wet-day precipitation and maximum five-day precipitation will be reported for each hydrometric area, and software will be provided to calculate indices aggregated over user-defined regions.

To understand the distribution of genuinely rare events - the type of precipitation events with an annual occurrence probability of at most 1 in 20 - extreme value theory will be used, as suggested by Klein Tank et al. (2009). Following Kharin et al. (2007), a generalised extreme value distribution (Coles et al., 2001) will be fitted to the sampled maximum precipitation values for each block (corresponding to the month, season or year of interest) within a twenty- or thirty-year window. The time slices to be reported are given in Table A1. As an alternative to this approach based on block maxima, in principle one could use a peaks-over-threshold (POT) methodology (Coles et al., 2001) to provide more precise characterisation of extremes; however, threshold selection for POT methods is hard to automate defensibly in nonstationary settings (AghaKouchak et al., 2012) - and automation is necessary when, as here, estimates are required for large numbers of time series. The quantiles of the fitted model will be used to infer the magnitude of a once-in-20-years precipitation event, and the change in 'return period' for current once-in-20-years precipitation events, for each time slice. The shape parameter of the fitted model, which controls the heaviness of the tails of the fitted distribution, will also be reported.

These indices will be produced for daily and five-day precipitation accumulations, both at individual grid cells and aggregated over the CEH hydrometric areas.

2.2.1 Definitions of precipitation indices

In defining the following indices of precipitation, let $\mathtt{pr}_{ij}$ be the daily precipitation amount in mm on day i in period j. $\{\mathtt{pr}_{ij} \geq 1\}$ denotes the subset of the $\{\mathtt{pr}_{ij}\}$ for which $\mathtt{pr}_{ij} \geq 1$.

Simple daily precipitation intensity index (SDII): Mean of $\{\mathtt{pr}_{ij} \geq 1\}$ in period j (Klein Tank et al., 2009).

Total precipitation: Sum of $\{\mathtt{pr}_{ij} \geq 1\}$ in period j (Klein Tank et al., 2009).

Maximum one-day precipitation: The maximum one-day precipitation for period j is $\max(\mathtt{pr}_{ij})$ (Klein Tank et al., 2009).

Maximum five-day accumulated precipitation: Let $\mathtt{pr}_{kj}$ be the total precipitation amount for the

five-day interval ending on day k in period j. The maximum five-day values for period j are $\max(\mathtt{pr}_{kj})$ (Klein Tank et al., 2009).

Proportion of convective precipitation: Let $\mathtt{prc}_{ij}$ be the daily precipitation amount due to convective rainfall on day i in period j. The proportion of total precipitation due to convective processes in period j is the sum of $\{\mathtt{prc}_{ij} \geq 1\}$ in period j divided by the total precipitation in period j.

Proportion of precipitation falling on days exceeding 95th percentile: Let $q_{95}(\mathtt{pr}_j)$ be the 95th percentile of daily wet-day precipitation during all seasons of interest (eg. during all winters) in the period j. The proportion of the total precipitation falling on days exceeding the 95th percentile in the season of interest for period j is the accumulation of precipitation falling on days on the precipitation exceeds $q_{95}(\mathtt{pr}_j)$ divided by the total accumulated precipitation for the same period and season (Klein Tank et al., 2009).

Proportion of precipitation falling on days exceeding 99th percentile: Let $q_{99}(\mathtt{pr}_j)$ be the 99th percentile of daily wet-day precipitation during all seasons of interest (eg. during all winters) in the period j. The proportion of the total precipitation falling on days exceeding the 99th percentile in the season of interest for period j is the accumulation of precipitation falling on days on the precipitation exceeds $q_{99}(\mathtt{pr}_j)$ divided by the total accumulated precipitation for the same period and season (Klein Tank et al., 2009).

Fraction of wet days: The proportion of days for which $\mathtt{pr}_{ij} \geq 1$ (Murphy et al., 2018).

Median length of dry spell: The median number of consecutive days in period j where $\mathtt{pr}_{ij} < 1$ (Maraun et al., 2015). Dry spells are assumed to occur in the season in which they finish.

Maximum length of dry spell: The largest number of consecutive days in period j where $\mathtt{pr}_{ij} < 1$ (ECA&D, 2020). Dry spells are assumed to occur in the season in which they finish.

Median length of wet spell: The median number of consecutive days in period j where $\mathtt{pr}_{ij} \geq 1$ (Maraun et al., 2015). Wet spells are assumed to occur in the season in which they finish.

Maximum length of wet spell: The largest number of consecutive days in period j where $\mathtt{pr}_{ij} \geq 1$ (ECA&D, 2020). Wet spells are assumed to occur in the season in which they finish.

Wet-dry transition probabilities: Let $P_j(ww)$ be the proportion of wet days in period j that are followed by a wet day, and let $P_j(dd)$ be the proportion of dry days in period j that are followed by a dry day, such that

$$P_j(ww) = \frac{\sum_{i=1}^{n} \mathbb{1}_{\{\mathtt{pr}_{ij} \geq 1\}} \mathbb{1}_{\{\mathtt{pr}_{i+1,j} \geq 1\}}}{\sum_{i=1}^{n} \mathbb{1}_{\{\mathtt{pr}_{ij} \geq 1\}}}, \qquad P_j(dd) = \frac{\sum_{i=1}^{n} \mathbb{1}_{\{\mathtt{pr}_{ij} < 1\}} \mathbb{1}_{\{\mathtt{pr}_{i+1,j} < 1\}}}{\sum_{i=1}^{n} \mathbb{1}_{\{\mathtt{pr}_{ij} < 1\}}},$$

where n is the total number of days in period j, and $\mathbb{1}_{\{\mathtt{pr}_{ij} > 1\}}$ is an indicator function with value one if $\mathtt{pr}_{ij} > 1$, and zero otherwise. The complementary transition probabilities are $P_j(wd) = 1 - P_j(ww)$ and $P_j(dw) = 1 - P_j(dd)$.

Magnitude of rare precipitation events: Let $\max(\mathtt{pr}_b)$ be the maximum precipitation in block b, where b may correspond to a single month, season, or year; and let $\{\max(\mathtt{pr}_b)\}$ be the set of all block maxima in the period of interest. A generalised extreme value distribution (GEV: Coles et al., 2001) is fitted to $\{\max(\mathtt{pr}_b)\}$; the 95th quantile of this fitted distribution is the 20-year return value (Kharin et al., 2007).

Return periods for current rare precipitation events: A GEV will be used to determine the magnitude of once-in-20-years daily precipitation for the reference period 1981–2010, as described above. A second GEV will be fitted to the future period of interest; then p denotes the probability under this future model that the reference 20-year return value will be exceeded. The return period $1/p$ will be reported for each future model (Kharin et al., 2007).

Parameters for distributions of extreme precipitation: The shape, location and tail parameters of the GEV distributions described above will be reported.

Magnitude, return period and shape parameters for extreme five-day precipitation: These are computed using the GEV method described above, but using block maxima of 5-day accumulated precipitation in place of 1-day precipitation.

2.3 Descriptive indices of wind

High winds during storms are responsible for greater insured losses over the UK than flood damage (Schwierz et al., 2010; Donat et al., 2011), while prolonged calm periods may result in low air quality, and in some regions may have implications for wind power generation. For this reason, indices quantifying these types of wind behaviour have been included in the set of descriptive indices used to characterise simulated climate variability. Definitions for calm and windy days are taken from ECA&D (2020), corresponding approximately to an average value on the Beaufort scale of 0-1 for calm days, and 6 or more for windy days; software will be provided for users to compute this index for any threshold. The maximum of the maximum sustained daily wind speed and of the maximum daily wind gust will also be reported for each period. The frequency of storms over the UK will be considered as part of the evaluation of physical plausibility in KA2.

2.3.1 Definitions of wind indices

In defining the following indices of wind speed, let $\texttt{sfcWind}_{ij}$ be the mean daily wind speed on day i in period j, let $\texttt{sfcWindmax}_{ij}$ be the maximum daily wind speed on day i in period j, and let $\texttt{wsgsmax}_{ij}$ be the maximum gust strength on day i in period j.

Number of windy days: The number of windy days in period j is the count of days where $\texttt{sfcWind}_{ij} \geq 10.8 ms^{-1}$ (ECA&D, 2020).

Number of calm days: The number of calm days in period j is the count of days where $\texttt{sfcWind}_{ij} \leq 2 ms^{-1}$ (ECA&D, 2020).

Maximum wind: The maximum sustained daily wind speed for period j is $\max(\texttt{sfcWindmax}_{ij})$ (ECA&D, 2020).

Maximum gust: The maximum daily gust speed for period j is $\max(\texttt{wsgsmax}_{ij})$.

Magnitude of rare high winds: Let $\max(\texttt{sfcWindmax}_b)$ be the maximum of the daily maximum wind speed in block b, where b may correspond to a single month, season, or year; and let $\{\max(\texttt{sfcWindmax}_b)\}$ be the set of all block maxima in the period of interest. A generalised extreme value distribution (GEV: Coles et al., 2001) is fitted to $\{\max(\texttt{sfcWindmax}_b)\}$; the 95th quantile of this fitted distribution is the 20-year return value (Kharin et al., 2007).

Return periods for current rare high wind speeds: A GEV will be used to determine the magnitude of once-in-20-years daily maximum wind speed for the reference period 1981–2010, as described

above. A second GEV will be fitted in the same way for the future period of interest; then p denotes the probability under this future model that the reference 20-year return value will be exceeded. The return period $1/p$ will be reported for each future model (Kharin et al., 2007).

Parameters for distributions of extreme precipitation: The shape, location and tail parameters of the GEV distributions described above will be reported.

Magnitude, return period and shape parameters for rare gust speeds: These are computed using the GEV method described above, but using block maxima of maximum gust speed `wsgsmax` in place of maximum sustained wind speed `sfcWindmax`.

2.4 Impact-relevant indices

Alongside summaries of the key variables listed in Fung et al. (2018) and the descriptive indices listed in Sections 2.1-2.3 above, selected indices of potentially high-impact weather will be computed. These particular indices have been chosen from a longer list suggested by the UKCP user group, covering six broad areas of interest:

Floods: Quantifying flood risks for specific areas requires complex hydrological modelling that is beyond the scope of this project, so no direct indices of flood risks are provided. However, the precipitation indices described in Section 2.2 are indicative of the changing risk of flooding across the UK, and software will be provided to support future impact studies by computing precipitation indices based on exceedances of user-specified thresholds.

Droughts: As with indices of flood risk, indices characterising drought risk in terms of minimum river flows require detailed hydrological modelling and are beyond the scope of this project. More general indices of meteorological drought risk are the standardised precipitation index (McKee et al., 1993, SPI), which models the probability of precipitation for a given accumulation period; and the standardised precipitation-evapotranspiration index (Vicente-Serrano et al., 2010, SPEI), which models the difference between precipitation and potential evapotranspiration (PET) in a given accumulation period. Although the Penman-Monteith method has been widely adopted as the standard procedure for computing the PET (Vicente-Serrano et al., 2010), the required meteorological data may not always be available; following the method used to produce the Centre for Ecology and Hydrology's historical gridded PET data product (Tanguy et al., 2017), the McGuinness-Bordne equation will be used in the computation of this index (McGuinness and Bordne, 1972; Oudin et al., 2005). The PET will be provided as a monthly time series for each of the hydrometric areas used in the precipitation reporting.

The SPEI computed from the previous six months' weather, denoted $SPEI_6$, has been shown to be a useful predictor of droughts in the UK (Parsons et al., 2019). $SPEI_6$ will be reported for each of the hydrometric areas used in the precipitation reporting, along with counts of drought events identified by particularly low values of the index. SPI_6, the SPI computed from the previous six months' weather, will also be reported.

Agricultural and agro-meteorological indices: For agricultural purposes, a key quantity is the soil moisture stress index β as reported in Murphy et al. (2018). However, calculation of this index would require extensive further modelling beyond the scope of this project (Best et al., 2011). As a proxy therefore, this project will report directly the mean soil moisture content at a depth of 1m, at daily and monthly time scales.

The UKCP user group suggested several indices to assess the agricultural impacts of projected changes in the climate. Of these, the annual growing season length will be reported, along with the annual total growing degree-days; both of these indices are computed with a threshold of 5.6°C, approximately the temperature at which grass starts to grow (Rivington et al., 2013; Harding et al., 2015). The growing degree days provide a measure of heat accumulation used to predict the development rates of plants and animals: for example, the date on which a particular species of flower will bloom, or a crop will reach maturity. Software will be provided to compute additional indices based on counts of temperatures relative to a given threshold, such as the number of frost days.

Energy demand: Heating and cooling degree-days are indices quantifying the need to heat or cool buildings, which act as a proxy for likely changes in energy usage under the projected scenarios (Azevedo et al., 2015). Default thresholds of 15.5°C for heating degree-days and 22°C for cooling degree-days will be used, with software provided to compute degree-days with user-specified thresholds.

Human comfort: The heat index (Steadman, 1979; Blazejczyk et al., 2012) combines the surface air temperature with the relative humidity to derive a human-perceived equivalent temperature. The maximum heat index will be reported for each period. The heat index is considered to be dangerously high when it exceeds 32°C, the threshold above which the National Oceanic and Atmospheric Administration advise extreme caution for people in high risk groups (Blazejczyk et al., 2012); the number of dangerously warm days will be reported for each period, together with numbers of tropical nights defined, following Klein Tank et al. (2009), as occasions on which the minimum temperature remains above 20°C.

Other risks: The UKCP user group suggested that the Met Office Fire Severity index (FSI) should be included in the final set of indices, to assess potentially increasing risks from wildfires. The FSI quantifies how severe a fire may become if one were to start (it does not quantify the risk of wildfires occurring). It is not clear whether all variables required as inputs to the FSI are available in the RCM output; if time permits and the supporting data is available, this index may be added to the analysis at a later stage.

2.4.1 Definitions of impact-relevant and user-focused indices

Potential evapo-transpiration (PET): The PET will be computed using the McGuinness-Bordne equation (McGuinness and Bordne, 1972; Tanguy et al., 2017),

$$PET = \frac{1}{\lambda} S_0 \left(\frac{T+5}{100} \right),$$

where λ is a constant representing the latent heat of vaporisation, T is the temperature in °C, and S_0 is the extraterrestrial radiation, estimated from the time of year and latitude. Calibration of the parameters λ and S_0 to accurately represent UK climate will be carried out after discussion with the authors of Tanguy et al. (2017).

Six-month standardised precipitation-evapotranspiration index ($SPEI_6$): The SPEI is the difference between the total precipitation and the PET in a given period (Vicente-Serrano et al., 2010). The index used will be $SPEI_6$, the SPEI computed each month for the preceding six months' weather conditions, as recommended by Parsons et al. (2019).

Drought duration: A drought event is deemed to begin in the month when the six-month standardised precipitation-evapotranspiration index falls below -1, and to end when it returns above 0 (McKee et al., 1993). Drought duration is the number of months during which a drought event is occurring (excluding the month in which the index returns to positive values) (Spinoni et al., 2014).

Mean soil moisture level: Let $\texttt{mrso}_{im}$ be the total soil moisture at a depth of 1m for day i in month m. The mean monthly soil moisture will be reported.

Growing season length: The growing season length for year y is the count of the number of days between the first occurrence of at least six consecutive days where $\texttt{tas}_{iy} > 5.6°\text{C}$ and the first occurrence after 1 July of at least six consecutive days where $\texttt{tas}_{iy} < 5.6°\text{C}$ (Rivington et al., 2013).

Growing degree-days: The number of growing degree-days in year y is $\sum_i \max(0, \texttt{tas}_{iy} - 5.6)$ (Rivington et al., 2013).

Cooling degree-days: The number of cooling degree-days in year y is $\sum_i \max(0, \texttt{tas}_{iy} - 22)$ (Azevedo et al., 2015).

Heating degree-days: The number of heating degree-days in year y is $\sum_i \max(0, 15.5 - \texttt{tas}_{iy})$ (Azevedo et al., 2015).

Daily heat index: Let T denote the daily maximum surface air temperature `tasmax` and R the relative humidity `hurs` for day i in period j. Then the heat index for day i in period j is

$$HI_{ij} = c_1 + c_2T + c_3R + c_4TR + c_5T^2 + c_6R^2 + c_7T^2R + c_8TR^2 + c_9T^2R^2$$

where the $\{c_i\}$ are constants as given in equation 1 of Blazejczyk et al. (2012). The heat index is only valid for air temperatures above 20°C and will be reported as NA when $T \leq 20°\text{C}$.

Number of days with dangerously high heat index: The number of days in period j on which the heat index is dangerously high is given by the count of $HI_{ij} \geq 32°\text{C}$ (Blazejczyk et al., 2012).

Number of tropical nights: Count the number of days where $\texttt{tasmin}_{ij} > 20°\text{C}$ (Klein Tank et al., 2009).

3 Physical plausibility (KA2)

The physical plausibility of the simulations will depend, in part, on how accurately the historical and evaluation runs are able to replicate the observed trends and variability in the KA1 descriptive indices described in Sections 2.1-2.3. Physical plausibility in the sense of how well the models represent the physical processes that drive the simulated climate will be evaluated in KA2 using indices characterising features of synoptic climatology that are relevant to UK weather. Where available, values of the KA2 indices will be taken from the CVDP data repository (Phillips et al., 2014).

The North Atlantic Oscillation (NAO) characterises the relative strengths and positions of the permanent low-pressure system over Iceland and the high-pressure system over the Azores, with a large difference in pressure between the two leading to increased westerly winds and consequent cool, wet summers and mild, wet winters in the UK; when the pressure gradient between the two systems is reduced, more extreme temperatures are observed over northern Europe, with hotter summers and colder, drier winters. The NAO is known to be one of the key drivers of variability in the weather over the UK, particularly in winter (Scaife et al., 2014). The NAO index will be computed using the principal component methodology of Hurrell and Deser (2010).

Extra-tropical cyclones over the UK bring high winds and extreme precipitation, and any projected changes in the North Atlantic storm track are likely to have significant impacts for the simulated weather over the UK. The position of the North Atlantic storm track, and the frequency of associated extra-tropical cyclones of the UK, will be evaluated for each of the EuroCORDEX models based on the methodology of Hodges et al. (2011).

The polar jet stream affects the speed with which storms pass over the UK; blocking events, which occur when the jet stream is prevented from following its climatological path, have been linked to recent extreme heatwaves in northern Europe and are associated with poor air quality due to low wind speeds and stagnant air (Barnes et al., 2012). It is therefore critical that the models are able to simulate both the latitude and strength of the jet stream, and also to produce blocking events with realistic magnitude and frequency. The position and strength of the jet stream in the EuroCORDEX GCMs will be quantified as described in Woollings et al. (2010); blocking events in the GCM output will be identified using the 'regime blocking method' proposed by Barnes et al. (2012). The strength of the stratospheric polar vortex, which is known to affect the strength of the polar jet stream, will also be computed, using the approach of Manzini et al. (2014) and Simpson et al. (2018).

Other synoptic features with potential relevance for UK weather are the Atlantic Multidecadal Oscillation (AMO), a cycle of multidecadal variability in North Atlantic sea surface temperatures that influences temperature and precipitation anomalies in many parts of the northern hemisphere, and in its warm phase drives wet summers over the UK (Sutton and Dong, 2012); and the Atlantic Meridional Overturning Circulation (MOC), which is characterised by a northward flow of warm water in the Atlantic, ameliorating the climate over Northwest Europe, including the UK (Menary et al., 2013). If time permits, the frequency of near-surface temperature inversions, which increase the likelihood of poor air quality, will be reported for each model.

Because computation of these synoptic-scale indices tends to be more involved than the simple thresholding used to define most of the KA1 indices characterising climate variability, precise details of the computation of each index of interest are not given in detail here; instead, Table 2 summarises the indices that will be reported, along with sources for the definitions that will be used.

Table 2: Indices of synoptic features to be computed for each GCM in the EuroCORDEX ensemble, along with the source for the methodology used.

Feature	**Source**
NAO index	Hurrell and Deser (2010)
Position of North Atlantic storm track	Hodges et al. (2011); Zappa et al. (2013)
Frequency of storms	
Jet stream strength	Woollings et al. (2010)
Jet stream latitude	
Strength of polar vortex	Manzini et al. (2014); Simpson et al. (2018)
Frequency of blocking events	Barnes et al. (2012)
Atlantic multidecadal oscillation (AMO)	Trenberth and Shea (2006)
Atlantic meridional overturning circulation (AMOC)	Danabasoglu et al. (2012)

The physical plausibility of the RCMs will be assessed by using patterns of mean sea level pressure (MSLP) anomalies from the driving GCMs to classify each day into one of a number of weather types, as described in Neal et al. (2016). As well as comparing the relative frequencies of the simulated weather types with those actually observed and evaluating changes in the frequency of each weather type over time, this analysis will consider the mean, within-weather-type variance, and inter-variable dependences of a subset of the KA1 variables characterising overall climate variability: the daily mean, minimum and maximum temperatures; the mean wet-day precipitation and count of wet days; the mean and maximum of the daily surface wind speed; and the relative humidity.

A Table of temporal resolutions

Indices will be computed from the EuroCORDEX simulations and presented as time series of varying resolutions, replicating the format of the publicly available UKCP18 data.

Daily means (day): The daily mean of each variable or index will be reported from 1980-12-01 to 2080-11-30 (length of time series will vary according to the calendar used in the driving model).

Monthly means (mon): Daily time series will be aggregated into months from 1980-12 to 2080-11 (1200 monthly means).

Seasonal means (seas): Monthly time series will be averaged over 3-month blocks corresponding to the seasons DJF, MAM, JJA, SON from DJF 1980 (December 1980 – February 1981) to SON 2080 (400 seasonal means).

Annual means (ann): Monthly time series will be averaged over 12-month blocks beginning on December 1st corresponding to the years 1981-2080, where the year 1981 denotes the period from December 1980 to November 1981 (100 annual means).

In addition, the monthly, seasonal and yearly time series for the core variables will be averaged over the 20- and 30-year time slices defined in Table A1, in line with the UKCP18 output. These time slices will also be used to compute the indices of extreme precipitation and wind described in Sections 2.2.1 and 2.3.1. The reference period used as the basis for computing climatological exceedances, and as the baseline against which changes will be reported in all project outputs, is the thirty-year period from December 1st 1980 to November 30th 2010, in line with recommendations from the World Meteorological Organisation (WMO, 2017): users should note that this differs from the twenty-year reference period used in the original UKCP18 analysis (Murphy et al., 2018).

Table A1: Definitions of time slices for which monthly, seasonal and annual averages of the core variables will be reported.

(a) Twenty-year time slices

Time slice	Start date	End date
1991	01-Dec-1980	30-Nov-2000
2000	01-Dec-1989	30-Nov-2009
2010	01-Dec-1999	30-Nov-2019
2020	01-Dec-2009	30-Nov-2029
2030	01-Dec-2019	30-Nov-2039
2040	01-Dec-2029	30-Nov-2049
2050	01-Dec-2039	30-Nov-2059
2060	01-Dec-2049	30-Nov-2069
2070	01-Dec-2059	30-Nov-2079

(b) Thirty-year time slices

Time slice	Start date	End date
1996	01-Dec-1980	30-Nov-2010
2005	01-Dec-1989	30-Nov-2019
2015	01-Dec-1999	30-Nov-2029
2025	01-Dec-2009	30-Nov-2039
2035	01-Dec-2019	30-Nov-2049
2045	01-Dec-2029	30-Nov-2059
2055	01-Dec-2039	30-Nov-2069
2065	01-Dec-2049	30-Nov-2079

B Map of hydrometric areas

Figure B1: Map of CEH hydrometric areas (National River Flow Archive, 2014) used to aggregate precipitation indices.

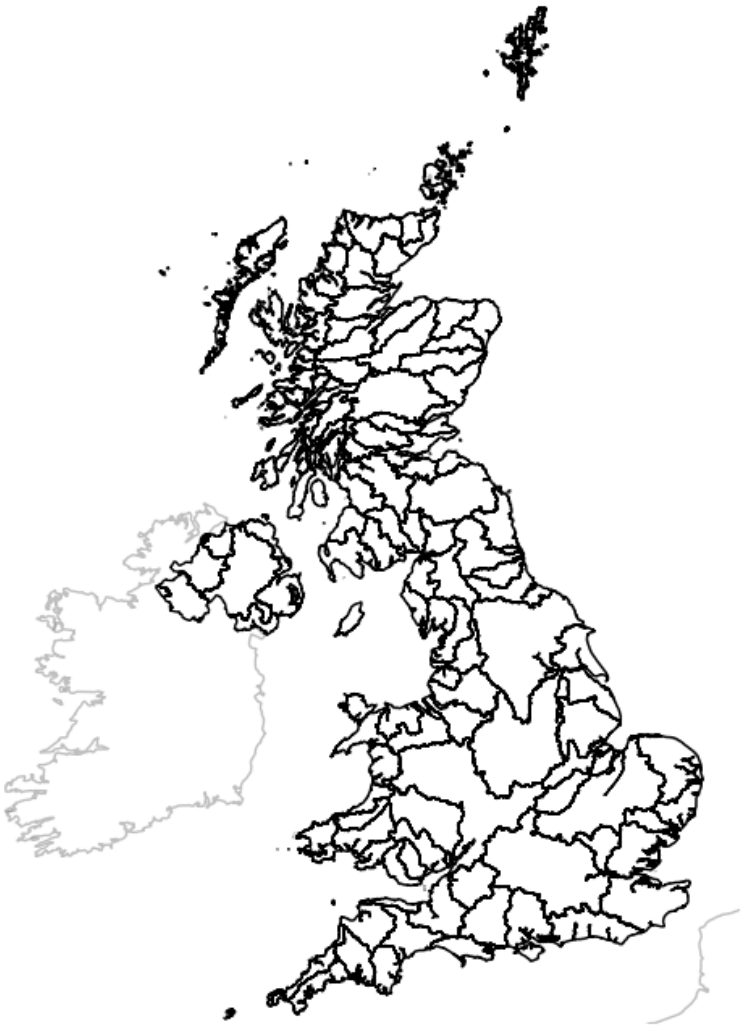

C Tables of KA1 indices

Table C1: UKCP18 core indices (Fung et al., 2018). Daily time series of all core indices will be provided, along with time series of monthly, seasonal and annual means. The mean of each core index will also be reported for each of the time slices defined in Table A1.

			Time series reported			
Index	**Code**	**Unit**	**day**	**mon**	**seas**	**ann**
Total cloud	clt	%	✓	✓	✓	✓
Relative humidity at 1.5m	hurs	%	✓	✓	✓	✓
Specific humidity at 1.5m	huss		✓	✓	✓	✓
Precipitation rate	pr	mm/day	✓	✓	✓	✓
Snowfall amount	prsn	mm/day	✓	✓	✓	✓
Sea level pressure	psl	hPa	✓	✓	✓	✓
Net surface long wave flux	rls	wm^{-2}	✓	✓	✓	✓
Net surface short wave flux	rss	wm^{-2}	✓	✓	✓	✓
Wind speed at 10m	sfcWind	ms^{-1}	✓	✓	✓	✓
Lying snow	snw	mm	✓	✓	✓	✓
Mean air temp at 1.5m	tas	°C	✓	✓	✓	✓
Max air temp at 1.5m	tasmax	°C	✓	✓	✓	✓
Min air temp at 1.5m	tasmin	°C	✓	✓	✓	✓
Eastward wind at 10m	uas	ms^{-1}	✓	✓	✓	✓
Northward wind at 10m	vas	ms^{-1}	✓	✓	✓	✓

Table C2: Indices of temperature defined in Section 2.1, showing the temporal resolutions at which each will be reported.

			Time series reported			
Index	**Code**	**Unit**	**day**	**mon**	**seas**	**ann**
Duration of cold spells	csdi	$days$	-	✓	✓	✓
Diurnal temperature range	dtr	°C	-	✓	✓	✓
Duration of heatwaves	hwdi	$days$	-	✓	✓	✓
Peak temperature	maxtmax	°C	-	✓	✓	✓
Temperature nadir	mintmin	°C	-	✓	✓	✓
Seasonal temperature range	str	°C	-	-	✓	✓
1st percentile of daily mean temps	tas01	°C	-	-	-	-
99th percentile of daily mean temps	tas99	°C	-	-	-	-
Number of cold days	tmax10p	$days$	-	✓	✓	✓
Number of warm days	tmax90p	$days$	-	✓	✓	✓
Number of cold nights	tmin10p	$days$	-	✓	✓	✓
Number of warm nights	tmin90p	$days$	-	✓	✓	✓

Table C3: Indices of precipitation defined in Section 2.2, showing the temporal resolutions at which each will be reported.

(a) Indices of non-extreme precipitation

			Time series reported			
Index	**Code**	**Unit**	**day**	**mon**	**seas**	**ann**
Maximum length of dry spell	`dsmax`	*days*	-	✓	✓	✓
Median length of dry spell	`dsmed`	*days*	-	✓	✓	✓
% of wet days	`fwd`	%	-	✓	✓	✓
% of dry days followed by a dry day	`pdd`	%	-	✓	✓	✓
Convective precipitation	`prc`	*mm/day*	✓	-	-	-
% of convective precipitation	`prcprop`	%	-	✓	✓	✓
Total precipitation	`prcptot`	*mm*	-	✓	✓	✓
% of wet days followed by a wet day	`pww`	%	-	✓	✓	✓
% of total precip exceeding q_{95}	`r95ptot`	%	-	✓	✓	✓
% of total precip exceeding q_{99}	`r99ptot`	%	-	✓	✓	✓
Maximum one-day precipitation	`rx1day`	*mm*	-	✓	✓	✓
Maximum five-day precipitation	`rx5day`	*mm*	-	✓	✓	✓
Simple daily intensity index	`sdii`	*mm*	-	✓	✓	✓
Maximum length of wet spell	`wsmax`	*days*	-	✓	✓	✓
Median length of wet spell	`wsmed`	*days*	-	✓	✓	✓

(b) Indices of extreme precipitation: these will be computed for each of the time slices defined in Table A1.

Index	**Code**	**Unit**
Magnitude of 1-in-20-year one-day precip	`rx1dayrl20`	*mm*
Return period for current 1-in-20-year one-day precip	`rx1dayrp20`	*years*
Magnitude of 1-in-50-year one-day precip	`rx1dayrl50`	*mm*
Return period for current 1-in-50-year one-day precip	`rx1dayrp50`	*years*
Location parameter for distribution of rare one-day events	`rx1dayloc`	*mm*
Shape parameter for distribution of rare one-day events	`rx1dayshape`	
Scale parameter for distribution of rare one-day events	`rx1dayscale`	
Magnitude of 1-in-20-year five-day precip	`rx5dayrl20`	*mm*
Return period for current 1-in-20-year five-day precip	`rx5dayrp20`	*years*
Magnitude of 1-in-50-year five-day precip	`rx5dayrl50`	*mm*
Return period for current 1-in-50-year five-day precip	`rx5dayrp50`	*years*
Location parameter for distribution of rare five-day events	`rx5dayloc`	*mm*
Shape parameter for distribution of rare five-day events	`rx5dayshape`	
Scale parameter for distribution of rare five-day events	`rx5dayscale`	

Table C4: Indices of wind defined in Section 2.3, showing the temporal resolutions at which each will be reported.

(a) Indices of non-extreme winds

Index	Code	Unit	Time series reported			
			day	mon	seas	ann
Maximum wind speed	`maxsfcWindmax`	ms^{-1}	-	✓	✓	✓
Maximum wind gust	`maxwsgsmax`	ms^{-1}	-	✓	✓	✓
Number of calm days	`ncalm`	*days*	✓	✓	✓	✓
Number of windy days	`nwindy`	*days*	✓	✓	✓	✓

(b) Indices of extreme winds: these will be computed for each of the time slices defined in Table A1.

Index	Code	Unit
Magnitude of 1-in-20-year wind speeds	`maxsfcWindmaxrl20`	ms^{-1}
Return period for current 1-in-20-year wind speeds	`maxsfcWindmaxrp20`	*years*
Magnitude of 1-in-50-year wind speeds	`maxsfcWindmaxrl50`	ms^{-1}
Return period for current 1-in-50-year wind speeds	`maxsfcWindmaxrp50`	*years*
Location parameter for distribution of extreme winds	`maxsfcWindmaxloc`	ms^{-1}
Shape parameter for distribution of extreme winds	`maxsfcWindmaxshape`	
Scale parameter for distribution of extreme winds	`maxsfcWindmaxscale`	
Magnitude of 1-in-20-year gusts	`maxwsgsmaxrl20`	ms^{-1}
Return period for current 1-in-20-year gusts	`maxwsgsmaxrp20`	*years*
Magnitude of 1-in-50-year gusts	`maxwsgsmaxrl50`	ms^{-1}
Return period for current 1-in-50-year gusts	`maxwsgsmaxrp50`	*years*
Location parameter for distribution of extreme winds	`maxwsgsmaxloc`	ms^{-1}
Shape parameter for distribution of extreme winds	`maxwsgsmaxshape`	
Scale parameter for distribution of extreme winds	`maxwsgsmaxscale`	

Table C5: Impact-relevant indices defined in Section 2.4, showing the temporal resolutions at which each will be reported.

Index	Code	Unit	Time series reported			
			day	mon	seas	ann
Cooling degree-days	`cdd`	$°days$	-	-	-	✓
Growing degree-days	`gdd`	$°days$	-	-	-	✓
Growing season length	`gsl`	*days*	-	-	-	✓
Heating degree-days	`hdd`	$°days$	-	-	-	✓
Heat index (HI)	`hi`	°C	✓	-	-	-
Mean soil moisture level at 1m	`mrso`	kgm^{-2}	✓	✓	-	-
Occurrences of dangerously high HI	`ndhi`	*days*	-	✓	✓	✓
Duration of of drought	`ndrought`	*months*	-	-	✓	✓
Potential evapo-transpiration	`pet`	mm/day	-	✓	-	-
$SPEI_6$	`spei6`		-	✓	-	-
SPI_6	`spi6`		-	✓	-	-
Number of tropical nights	`tr`	*days*	-	✓	✓	✓

References

AghaKouchak, A., Easterling, D., Hsu, K., Schubert, S., and Sorooshian, S. (2012). *Extremes in a changing climate: detection, analysis and uncertainty*, volume 65. Springer Science & Business Media.

Arnell, N., Kay, A., Freeman, A., Rudd, A., and Lowe, J. (2021). Changing climate risk in the UK: a multi-sectoral analysis using policy-relevant indicators. *Climate Risk Management*, 31:100265.

Azevedo, J. A., Chapman, L., and Muller, C. L. (2015). Critique and suggested modifications of the degree days methodology to enable long-term electricity consumption assessments: a case study in Birmingham, UK. *Meteorological Applications*, 22(4):789–796.

Barnes, E. A., Slingo, J., and Woollings, T. (2012). A methodology for the comparison of blocking climatologies across indices, models and climate scenarios. *Climate dynamics*, 38(11-12):2467–2481.

Best, M., Pryor, M., Clark, D., Rooney, G., Essery, R., Ménard, C., Edwards, J., Hendry, M., Porson, A., Gedney, N., et al. (2011). The Joint UK Land Environment Simulator (JULES), model description–Part 1: energy and water fluxes. *Geoscientific Model Development*, 4(3):677–699.

Blazejczyk, K., Epstein, Y., Jendritzky, G., Staiger, H., and Tinz, B. (2012). Comparison of UTCI to selected thermal indices. *International journal of biometeorology*, 56(3):515–535.

Coles, S., Bawa, J., Trenner, L., and Dorazio, P. (2001). *An introduction to statistical modeling of extreme values*, volume 208. Springer.

Danabasoglu, G., Yeager, S. G., Kwon, Y.-O., Tribbia, J. J., Phillips, A. S., and Hurrell, J. W. (2012). Variability of the Atlantic meridional overturning circulation in CCSM4. *Journal of climate*, 25(15):5153–5172.

Donat, M., Leckebusch, G., Wild, S., and Ulbrich, U. (2011). Future changes in European winter storm losses and extreme wind speeds inferred from GCM and RCM multi-model simulations. *Natural Hazards and Earth System Sciences*, 11(5):1351–1370.

ECA&D (2020). European Climate Assessment & Dataset project. https://www.ecad.eu/indicesextremes/.

Fung, F., Stephens, A., and Wilson, A. (2018). UKCP18 Guidance: Data availability, access and formats. *Met Office Hadley Centre: Exeter, UK*.

Hajat, S., Vardoulakis, S., Heaviside, C., and Eggen, B. (2014). Climate change effects on human health: projections of temperature-related mortality for the UK during the 2020s, 2050s and 2080s. *J Epidemiol Community Health*, 68(7):641–648.

Harding, A., Rivington, M., Mineter, M., and Tett, S. (2015). Agro-meteorological indices and climate model uncertainty over the UK. *Climatic Change*, 128(1):113–126.

Hodges, K. I., Lee, R. W., and Bengtsson, L. (2011). A comparison of extratropical cyclones in recent re-analyses ERA-Interim, NASA MERRA, NCEP CFSR, and JRA-25. *Journal of Climate*, 24(18):4888–4906.

Hurford, A., Priest, S., Parker, D., and Lumbroso, D. (2012). The effectiveness of extreme rainfall alerts in predicting surface water flooding in England and Wales. *International journal of climatology*, 32(11):1768–1774.

Hurrell, J. W. and Deser, C. (2010). North Atlantic climate variability: the role of the North Atlantic Oscillation. *Journal of marine systems*, 79(3-4):231–244.

Kennedy-Asser, A. T., Andrews, O., Mitchell, D. M., and Warren, R. F. (2021). Evaluating heat extremes in the UK Climate Projections (UKCP18). *Environmental Research Letters*, 16(1):014039.

Kharin, V. V., Zwiers, F. W., Zhang, X., and Hegerl, G. C. (2007). Changes in temperature and precipitation extremes in the IPCC ensemble of global coupled model simulations. *Journal of Climate*, 20(8):1419–1444.

Klein Tank, A. M., Zwiers, F. W., and Zhang, X. (2009). Guidelines on analysis of extremes in a changing climate in support of informed decisions for adaptation. *World Meteorological Organization*.

Manzini, E., Karpechko, A. Y., Anstey, J., Baldwin, M., Black, R., Cagnazzo, C., Calvo, N., Charlton-Perez, A., Christiansen, B., Davini, P., et al. (2014). Northern winter climate change: assessment of uncertainty in CMIP5 projections related to stratosphere-troposphere coupling. *Journal of Geophysical Research: Atmospheres*, 119(13):7979–7998.

Maraun, D., Widmann, M., Gutiérrez, J. M., Kotlarski, S., Chandler, R. E., Hertig, E., Wibig, J., Huth, R., and Wilcke, R. A. (2015). VALUE: A framework to validate downscaling approaches for climate change studies. *Earth's Future*, 3(1):1–14.

McGuinness, J. and Bordne, E. (1972). A comparison of lysimeter derived potential evapotranspiration with computed values. *Agric. Res. Serv., US Dep. of Agric., Washington, DC*.

McKee, T. B., Doesken, N. J., Kleist, J., et al. (1993). The relationship of drought frequency and duration to time scales. In *Proceedings of the 8th Conference on Applied Climatology*, volume 17, pages 179–183. Boston.

Meehl, G. A. and Tebaldi, C. (2004). More intense, more frequent, and longer lasting heat waves in the 21st century. *Science*, 305(5686):994–997.

Menary, M. B., Roberts, C. D., Palmer, M. D., Halloran, P. R., Jackson, L., Wood, R. A., Müller, W. A., Matei, D., and Lee, S.-K. (2013). Mechanisms of aerosol-forced AMOC variability in a state of the art climate model. *Journal of Geophysical Research: Oceans*, 118(4):2087–2096.

Murphy, J., Harris, G., Sexton, D., Kendon, E., Bett, P., Clark, R., Eagle, K., Fosser, G., Fung, F., Lowe, J., et al. (2018). UKCP18 land projections: science report. *Met Office*.

National River Flow Archive (2014). Integrated Hydrological Units of the United Kingdom: Hydrometric areas with coastline.

Neal, R., Fereday, D., Crocker, R., and Comer, R. E. (2016). A flexible approach to defining weather patterns and their application in weather forecasting over Europe. *Meteorological Applications*, 23(3):389–400.

Oudin, L., Hervieu, F., Michel, C., Perrin, C., Andréassian, V., Anctil, F., and Loumagne, C. (2005). Which potential evapotranspiration input for a lumped rainfall–runoff model?: Part 2–towards a simple and efficient potential evapotranspiration model for rainfall–runoff modelling. *Journal of hydrology*, 303(1-4):290–306.

Palin, E. J., Thornton, H. E., Mathison, C. T., McCarthy, R. E., Clark, R. T., and Dora, J. (2013). Future projections of temperature-related climate change impacts on the railway network of Great Britain. *Climatic Change*, 120(1):71–93.

Parsons, D. J., Rey, D., Tanguy, M., and Holman, I. P. (2019). Regional variations in the link between drought indices and reported agricultural impacts of drought. *Agricultural systems*, 173:119–129.

PHE (2018). Cold weather plan for England. https://www.gov.uk/government/publications/cold-weather-plan-cwp-for-england.

PHE (2020). Heatwave plan for England. https://www.gov.uk/government/publications/heatwave-plan-for-england.

Phillips, A. S., Deser, C., and Fasullo, J. (2014). Evaluating modes of variability in climate models. *Eos, Transactions American Geophysical Union*, 95(49):453–455.

Rivington, M., Matthews, K. B., Buchan, K., Miller, D., Bellocchi, G., and Russell, G. (2013). Climate change impacts and adaptation scope for agriculture indicated by agro-meteorological metrics. *Agricultural Systems*, 114:15–31.

Scaife, A., Arribas, A., Blockley, E., Brookshaw, A., Clark, R., Dunstone, N., Eade, R., Fereday, D., Folland, C., Gordon, M., et al. (2014). Skillful long-range prediction of European and North American winters. *Geophysical Research Letters*, 41(7):2514–2519.

Schwierz, C., Köllner-Heck, P., Mutter, E. Z., Bresch, D. N., Vidale, P.-L., Wild, M., and Schär, C. (2010). Modelling European winter wind storm losses in current and future climate. *Climatic change*, 101(3):485–514.

Simpson, I. R., Hitchcock, P., Seager, R., Wu, Y., and Callaghan, P. (2018). The downward influence of uncertainty in the northern hemisphere stratospheric polar vortex response to climate change. *Journal of Climate*, 31(16):6371–6391.

Spinoni, J., Naumann, G., Carrao, H., Barbosa, P., and Vogt, J. (2014). World drought frequency, duration, and severity for 1951–2010. *International Journal of Climatology*, 34(8):2792–2804.

Steadman, R. G. (1979). The assessment of sultriness. Part I: A temperature-humidity index based on human physiology and clothing science. *Journal of Applied Meteorology and Climatology*, 18(7):861–873.

Sutton, R. T. and Dong, B. (2012). Atlantic Ocean influence on a shift in European climate in the 1990s. *Nature Geoscience*, 5(11):788–792.

Tanguy, M., Prudhomme, C., Smith, K., and Hannaford, J. (2017). Historic Gridded Potential Evapotranspiration (PET) based on temperature-based equation McGuinness-Bordne calibrated for the UK (1891–2015). *NERC Environmental Information Data Centre*, 10.

Trenberth, K. E. and Shea, D. J. (2006). Atlantic hurricanes and natural variability in 2005. *Geophysical research letters*, 33(12).

Vicente-Serrano, S. M., Beguería, S., and López-Moreno, J. I. (2010). A multiscalar drought index sensitive to global warming: the standardized precipitation evapotranspiration index. *Journal of climate*, 23(7):1696–1718.

WMO (2017). WMO guidelines on the calculation of climate normals. World Meteorological Organization Geneva, Switzerland.

Wood, F. R., Calverley, D., Glynn, S., Mander, S., Conor, W., Kuriakose, J., Hill, F., and Roeder, M. (2015). The impacts of climate change on UK energy demand. *Infrastructure Asset Management*, 2(3):107–119.

Woollings, T., Hannachi, A., and Hoskins, B. (2010). Variability of the North Atlantic eddy-driven jet stream. *Quarterly Journal of the Royal Meteorological Society*, 136(649):856–868.

Zappa, G., Shaffrey, L. C., Hodges, K. I., Sansom, P. G., and Stephenson, D. B. (2013). A multimodel assessment of future projections of North Atlantic and European extratropical cyclones in the CMIP5 climate models. *Journal of Climate*, 26(16):5846–5862.